Available online at www.sciencedirect.com
ScienceDirect
Solar Energy 85 (2011) 2407–2420
SOLAR ENERGY
www.elsevier.com/locate/solener

Techno-economic valuation and optimization of integrated photovoltaic/wind energy conversion system

Abdelhamid Kaabeche [a,*], Maïouf Belhamel [a], Rachid Ibtiouen [b]

[a] Centre de Développement des Energies Renouvelables, B.P. 62, 16340 Bouzareah, Algiers, Algeria
[b] Ecole Nationale Supérieure Polytechnique d'El Harrach, Algiers, Algeria

Received 13 January 2011; received in revised form 24 March 2011; accepted 7 June 2011

Communicated by: Associate Editor Mukund Patel

Abstract

Decentralized electricity generation by renewable energy sources offer greater security of supply for consumers while respecting the environment. But the random nature of these sources requires us to develop sizing rules and use these systems to exploit them. This paper proposes an integrated PV/wind hybrid system optimization model, which utilizes the iterative optimization technique following the Deficiency of Power Supply Probability (DPSP), the Relative Excess Power Generated (REPG), the Total Net Present Cost (TNPC), the Total Annualized Cost (TAC) and Break-Even Distance Analysis (BEDA) for power reliability and system costs. The flow chart of the hybrid optimal sizing model is also illustrated. With this merged model, the optimal size of PV/wind hybrid energy conversion system using battery bank can be performed technically and economically according to the system reliability requirements. Additionally, a sensitivity analysis was carried out in order to appreciate the most important parameters influencing the economic performances of the hybrid system. A case study is conducted to analyze one hybrid project, which is designed to supply small residential household situated in the area of the Center for Renewable Energy Development (CDER) localized in Bouzaréah, Algeria (36°48′N, 3°1′E, 345 m).

Keywords: Renewable energy system; Unit sizing; Economic viability; Optimization

1. Introduction

Energy generation is a challenge of great importance for years to come. Indeed, the energy needs of industrialized societies are increasing, moreover, developing countries will need more energy to complete their development. Consumption of these sources leads to emissions of greenhouse gases and thus increasing pollution. The rapid depletion and price volatility of fossil fuels worldwide have necessitated urgent search for new energy sources to meet current requirements.

Alternative energy resources such as hydropower, wind, solar and geothermal have attracted energy sectors to generate power on a large scale. However, common drawback with solar and wind energy is their unpredictable nature and dependence on weather and climatic changes, and the variations of solar and wind energy may not match with the time distribution of load demand. This short-coming not only affects the system's energy performance, but also results in batteries being discarded too early. Generally, the independent use of both energy resources may result in considerable over-sizing, which in turn makes the design costly. It is prudent that neither a stand-alone solar energy system nor a wind energy system can provide a continuous power supply due to seasonal and periodical variations (Yang et al., 2008) for stand-alone systems.

In order to efficiently and economically utilize the renewable energy resources, one optimum match design sizing method is essential. The sizing optimization method can help

* Corresponding author. Fax: +213 21 90 15.
E-mail address: h.kaabeche@hotmail.com (A. Kaabeche).

0038-092X/$ - see front matter © 2011 Elsevier Ltd. All rights reserved.
doi:10.1016/j.solener.2011.06.032

to endorse the lowest investment with adequate and full use of the renewable energy systems (photovoltaic, wind, thermal systems, etc.). Thus, Chel et al. (2009) presented the methodology to evaluate size and cost of PV power system components. The PV array size is determined based on daily electrical load and number of sunshine hours on optimally tilted surface specific to the country. Based on life cycle cost (LCC) analysis, capital cost (US$/kW$_P$) and unit cost of electricity (US$/kW h) were determined for PV systems such as stand-alone PV (SAPV) and building integrated PV (BIPV). Effect of carbon credit on the economics of PV system showed reduction in unit cost of electricity for SAPV and BIPV systems, respectively. The developed methodology was illustrated using actual case study on 2.32 kW$_P$ PV system located in New Delhi (India).

Another study on performance evaluation of 2.32 kW$_P$ photovoltaic (PV) power system located in New Delhi (India) has been performed by Chel and Tiwari (2010). The considered PV system feeds an electric air blower of an earth to air heat exchanger (EAHE) used for heating/cooling of adobe house, computer, submersible water pump, etc. The outdoor efficiencies, power generated and lost in PV system components were determined using hourly experimental measured data for 1 year on typical clear day in each month. The energy conservation, mitigation of CO_2 emission and carbon credit potential of the existing PV integrated EAHE system is presented too. Also, the energy payback time (EPBT) and unit cost of electricity were determined for both stand-alone PV (SAPV) and building roof integrated PV (BIPV) systems.

One more experimental outdoor performance of a 2.32 kW$_P$ stand-alone photovoltaic (SAPV) system for four weather types have been performed by Chel and Tiwari (2011). The number of days and daily power generated corresponding to four weather types in each month were used to determine monthly and subsequently annual power generation from the existing SAPV system. There are three daily load profiles with and without earth to air heat exchanger suitable for three seasons like summer, winter and rainy. The life cycle cost (LCC) analysis for the existing typical SAPV system is carried out to determine unit cost of electricity. The effect of annual degradation rate of PV system efficiency is also presented.

A performance experiments and economic analysis of a horizontal ground source heat pump (GSHP) system have been performed by Esen et al. (2006). The GSHP system was compared to conventional heating methods (electric resistance, fuel oil, liquid petrol gas, coal, oil and natural gas) in the economical analysis using an annualized life cycle cost method. It was shown that the GSHP system offers economic advantages over the mentioned first five conventional heating methods. However, it is not an economic alternative system to natural gas. Another techno-economic comparison between a ground-coupled heat pump (GCHP) system and an air-coupled heat pump (ACHP) system has been presented by Esen et al. (2007). The test results indicate that system parameters can have an important effect on performance, and that GCHP systems are economically preferable to ACHP systems for the purpose of space cooling.

A graphical construction technique to follow the optimum combination of PV array and battery bank for a hybrid solar–wind system has been presented by Borowy and Salameh (1996). For a given load and a desired LPSP, the number of batteries and PV modules were calculated based on the minimum cost of the system. The minimum cost will be at the point of tangency of the curve that represents the relationship between the number of PV modules and the number of batteries. Another graphical technique has been given by Ai et al. (2003), Kaabeche et al. (2006) and Markvart (1996), to optimally design a hybrid solar–wind power generation system.

Tina et al. (2006) presented a probabilistic approach based on the convolution technique (Karaki et al., 1999) to incorporate the fluctuating nature of the resources and the load, thus eliminating the need for time-series data, to assess the long-term performance of a hybrid solar–wind system for both stand-alone and grid-connected applications. Yang et al. (2008) proposed one optimum sizing method based on Genetic Algorithms by using the Typical Meteorological Year data. This optimization model is proposed to calculate the system optimum configuration which can achieve the desired LPSP with minimum Annualized Cost of System. Another heuristic technique based on the evolutionary algorithms have been performed by Ekren and Ekren (2010) for optimizing size of a PV/wind integrated hybrid energy system with battery storage. In the study, the objective function is the minimization of the hybrid energy system total cost.

Bernal-Agustín et al. (2006) present a multi-objective optimization (NPC versus CO_2 emissions) for a hybrid solar/wind/diesel system with battery storage based on Multi-Objective Evolutionary Algorithms (MOEAs). A triple multi-objective optimization to minimize simultaneously the total cost throughout the useful life of the installation, pollutant emissions (CO_2) and unmet load has been presented by Dufo-López and Bernal-Agustín (2008). For this task, a MOEAs and a Genetic Algorithm have been used in order to find the best combination of components and control strategies for the hybrid system. According to the methods proposed by Chedid and Rahman (1997) and Yokoyama et al. (1994) the optimal sizes of the PV and wind power sources and the batteries are determined by minimizing the system total cost function using linear programming techniques. The total system cost consists of both the initial cost and yearly operation and maintenance costs.

Yang et al. (2003, 2007) have proposed an iterative optimization technique following the loss of power supply probability (LPSP) model for a hybrid solar–wind system. The number selection of the PV module, wind turbine and battery ensures the load demand according to the power reliability requirement, and the system cost is minimized. Another iterative optimization technique to optimize the

capacity sizes of different components of hybrid photovoltaic/wind power generation system using a battery bank has been presented by Kaabeche et al. (2010). The recommended methodology takes into account the submodels of the hybrid system, the Deficiency of Power Supply Probability (DPSP) and the Levelised Unit Electricity Cost (LUEC). With the recommended iterative optimization method, the sizing optimization of grid-independent hybrid PV/wind power generation system can be accomplished technically and economically according to the system reliability requirements. Similarly, an iterative optimization technique for a stand-alone hybrid photovoltaic/wind system (HPWS) with battery storage is presented by Diaf et al. (2008a). The main objective of the presented study is to find the optimum size of system, able to fulfill the energy requirements of a given load distribution, for three sites located at Corsica island and to analyze the impact of different parameters on the system size.

In this paper, an integrated photovoltaic/wind hybrid system optimization model, which utilizes the iterative optimization technique following the Deficiency of Power Supply Probability (DPSP), the Relative Excess Power Generated (REPG), the Total Net Present Cost (TNPC), the Total Annualized Cost (TAC) and Break-Even Distance Analysis (BEDA) for power reliability and system costs, has been presented. The developed model permits also, the calculation of the excess energy. So, the surplus energy produced could be used in the production of hydrogen from an electrolyzer for long-term energy storage, helping to improve the total efficiency of the hybrid system. Additionally, a sensitivity analysis was carried out in order to appreciate the most important parameters influencing the economic performances of the hybrid system. A simulation software code has been developed to size system components in order to meet the load demand in the most cost effective way.

2. Integrated system description

A schematic diagram of a stand-alone hybrid PV/wind system is shown in Fig. 1. This integrated PV/wind hybrid system consists of PV subsystem, wind power subsystem, battery bank, power conditioners, inverter, controller and other accessory devices and cables. The PV generator and wind turbine operate conjointly to meet the load demand. When production conditions (wind speed and solar radiation) are available, the generated power, after satisfying the load demand, will be supplied to feed the battery until it is full charged. On the contrary, when production conditions are weak, the battery bank will be used to cover the energy deficit between production and demand until the state of charge of battery bank decreases to its minimum level.

3. Hybrid PV/wind system model

In order to predict the hybrid system performance, individual components need to be modeled first and then their mix can be evaluated to meet the load demand. The methodology for modeling hybrid PV/wind system components is described below.

3.1. Photovoltaic system model

The input energy to PV system is solar radiation and global solar irradiance, $G_{G,tilt}$, received on a tilted surface can be evaluated from the classic equation (Posadillo and López Luque, 2009):

$$G_{G,tilt} = G_{dir,tilt} + G_{diff,tilt} + G_{refl,tilt} \quad (1)$$

where $G_{dir,tilt}$, $G_{diff,tilt}$ and $G_{refl,tilt}$ are the hourly direct, sky-diffuse and ground reflected irradiance on the tilted surface. These components are calculated from hourly global solar irradiation $G_{G,hor}$ on a horizontal plane. The diffuse irradiance on a tilted surface, $G_{diff,tilt}$, is given by Klucher (1979):

$$G_{diff,tilt} = \left[G_{diff,hor}\frac{1+\cos\beta}{2}\right]\left[1+F\sin^3\left(\frac{\beta}{2}\right)\right] \times \left[1+F\cos^2\theta\cos^3\theta_Z\right] \quad (2)$$

where $G_{diff,hor}$ is the horizontal diffuse solar radiation; β is the slop angle of the PV module; θ is solar incidence angle on a tilted surface; θ_z is the zenith angle and F is the modulating function given by:

$$F = 1 - (M_d)^2 \quad (3)$$

With M_d the diffuse fraction defined by the following relation:

$$M_d = G_{diff,hor}/G_{G,hor} \quad (4)$$

where $G_{G,hor}$ is the global solar irradiation on a horizontal plane.

The KTCORAlger model (Chikh et al., 2000) is used for estimating hourly diffuse irradiance on a horizontal surface from hourly global irradiance $G_{G,hor}$. For three different ranges of atmospheric transmissivity, the resulting correlations are given by the following expression:

$$\frac{G_{diff,hor}}{G_{G,hor}} = \begin{cases} M_d = 1 - 0.14M_t - 0.037\sin(\alpha) & \text{for } 0 \le M_t \le 0.175 \\ M_d = 1 - 0.43M_t - 0.237\sin(\alpha) & \text{for } 0.175 \le M_t \le 0.87 \\ M_d = 0.23M_t - 0.74\sin(\alpha) & \text{for } M_t > 0.175 \end{cases} \quad (5)$$

where $\sin(\alpha)$ is the sun elevation and M_t the hourly clearness index given by Notton et al. (2010):

$$M_t = G_{G,hor}/G_{extr,hor} \quad (6)$$

where $G_{extr,hor}$ is the hourly extraterrestrial solar irradiance on a horizontal surface.

The direct irradiance on a tilted surface, $G_{dir,tilt}$, is related to the direct irradiance on horizontal surface, $G_{dir,hor}$, as follows (Mehleri et al., 2010):

$$G_{dir,tilt} = G_{dir,hor}\frac{\cos\theta}{\cos\theta_Z} \quad (7)$$

The direct irradiance on horizontal surface, $G_{dir,hor}$, can be calculated as follows:

$$G_{dir,hor} = G_{G,hor} - G_{diff,hor} \quad (8)$$

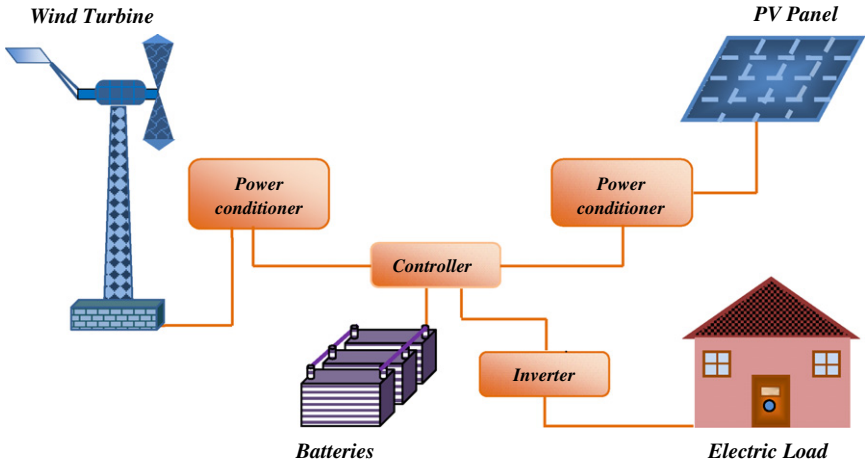

Fig. 1. Block diagram of a hybrid PV/wind system.

The ground reflectance irradiance on a tilted surface, $G_{refl,tilt}$, is related to the global irradiance on a horizontal surface, $G_{G,hor}$, by (Iqbal, 1983):

$$G_{refl,tilt} = \rho \frac{G_{G,hor}(1-\cos\beta)}{2} \tag{9}$$

We have assumed the value of "ρ" equal to 0.2 in the calculation conducted.

Hourly power output from PV system with an area A_{PV} (m^2), when total solar irradiance of $G_{G,tilt}$ (W/m^2) is incident on PV surface, is given by Markvar (2000):

$$P_{PV} = \eta_{PV} A_{PV} G_{G,tilt} \tag{10}$$

where η_{PV} represents the PV generator efficiency and is given by Habib et al. (1999) and Kolhe et al. (2003):

$$\eta_{PV} = \eta_r \eta_{pc}[1-\mu(\theta_{cell}-\theta_{cell,ref})] \tag{11}$$

where η_r is the reference module efficiency, η_{pc} is the power conditioning efficiency which is equal to 1 if a perfect maximum power tracker (MPPT) is used. μ is the generator efficiency temperature coefficient, it is assumed to be a constant and for silicon cells the range of μ is 0.004–0.006 per (°C), $\theta_{cell,ref}$ is the reference cell temperature (°C) and θ_{cell} is the cell temperature (°C) and can be calculated as follows (Diaf et al., 2008b):

$$\theta_{cell} = \theta_a + [(NOCT-20)/800]G_{G,tilt} \tag{12}$$

where θ_a is the ambient temperature (°C) and $NOCT$ is the nominal cell operating temperature (°C). η_{pc}, μ, $NOCT$ and A_{PV}, are parameters that depend upon the type of module used. The data are obtained from the PV module manufacturers.

3.2. Wind turbine system model

Power output of wind turbine generator at a specific site depends on wind speed at hub height and speed characteristics of the turbine. Wind speed at hub height can be calculated by using power-law equation (Kaviani et al., 2009; Belfkira et al., 2011):

$$\frac{V(H)}{V(H_{ref})} = \left(\frac{H}{H_{ref}}\right)^{\propto} \tag{13}$$

where $V(H)$ and $V(H_{ref})$ are the wind speed at hub and reference height H and H_{ref} and α is roughness coefficient. The value of the coefficient varies from less than 0.10 for very flat land, water or ice to more than 0.25 for heavily forested landscapes. The one-seventh power law (0.14) is a good reference number for relatively flat surfaces such as the open terrain of grasslands away from tall trees or buildings (Kaviani et al., 2009). Fig. 2 shows typical wind turbine characteristics. Power output of a wind energy conversion system $P_W(V)$ can be calculated as follows (Wen et al., 2009).

$$P_w(V) = \begin{cases} P_R(A+BV+CV^2), & V_c \le V \le V_R \\ P_R, & V_R \le V \le V_F \\ 0, & \text{otherwise} \end{cases} \tag{14}$$

The constants A, B and C are found out using the following equations:

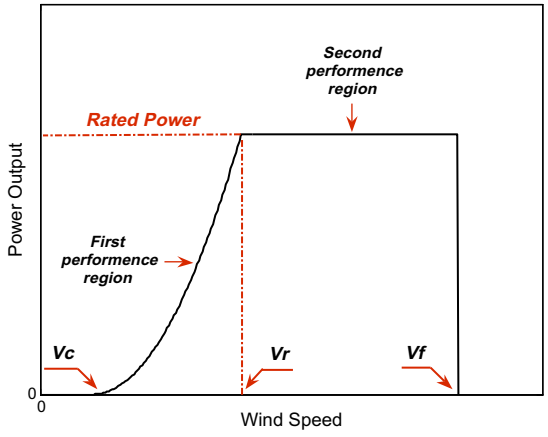

Fig. 2. A typical wind turbine output characteristics.

$$A = \frac{1}{V_C^2 - V_R^2}\left[V_C(V_C + V_R) - 4(V_C V_R)\left(\frac{(V_C + V_R)}{2V_R}\right)^3\right] \quad (15)$$

$$B = \frac{1}{V_C^2 - V_R^2}\left[4(V_C + V_R)\left(\frac{(V_C + V_R)}{2V_R}\right)^3 - 3(V_C + V_R)\right] \quad (16)$$

$$C = \frac{1}{V_C^2 - V_R^2}\left[2 - 4\left(\frac{(V_C + V_R)}{2V_R}\right)^3\right] \quad (17)$$

Generally, the cut-in speed of a wind turbine is in the range of 2.5–3.5 m/s and cut-out speed is in the range of 20–25 m/s.

3.3. Battery bank system model

Battery bank storage is sized to meet the load demand during non-availability period of renewable energy source, commonly referred to as days of autonomy. Normally the number of days of autonomy is taken to be 2 or 3 days. Battery sizing depends on factors such as maximum depth of discharge, temperature correction, rated battery capacity and battery life. The total capacity of the battery bank that is to be employed to meet the load is determined using the following expression (Deshmukh and Deshmukh, 2008):

$$C_B = \frac{E_L S_D}{V_B (DOD)_{\max} T_{cf} \eta_B} \quad (18)$$

where E_L is the load in Wh; S_D is the battery autonomy or storage days; V_B is the battery bank voltage; $DOD_{\max}$ is the maximum battery depth of discharge; T_{cf} is the temperature correction factor and η_B is the battery efficiency.

Depending on the PV and wind energy production and the load power requirements, the state of charge of battery can be calculated from the following equations:

Battery charging,

$$SOC(t) = SOC(t-1)\cdot(1-\sigma) + [E_{Gen}(t) - E_L(t)/\eta_{inv}]\cdot\eta_B \quad (19)$$

Battery discharging,

$$SOC(t) = SOC(t-1)\cdot(1-\sigma) + [E_L(t)/\eta_{inv} - E_{Gen}(t)] \quad (20)$$

where $SOC(t)$ and $SOC(t-1)$ are the states of charge of battery bank (Wh) at the time t and $t-1$, respectively; σ is hourly self-discharge rate; $E_{Gen}(t)$ is the total energy generated by PV array and wind generators after energy loss of controller; $E_L(t)$ is load demand at the time t; η_{inv} and η_B are the efficiency of inverter and charge efficiency of battery bank, respectively. At any time t, the charged quantity of the battery bank is subject to the following two constraints:

$$SOC_{\min} \leqslant SOC(t) \leqslant SOC_{\max} \quad (21)$$

the maximum charge quantity of battery bank $SOC_{\max}$ takes the value of nominal capacity of battery bank C_B, and the minimum charge quantity of battery bank $SOC_{\min}$, is determined by the maximum depth of discharge (DOD): $SOC_{\min} = (1 - DOD)\cdot C_B$. According to the specifications from the manufacturers, the battery's lifetime can be prolonged to the maximum if DOD takes the value of 30–50%. In this paper, the DOD takes the value of 50%.

4. Optimal sizing criteria for hybrid renewable energy system

In the existing literature there are various methods to evaluate the hybrid PV/wind energy system (HPWES) such as energy to load ratio, battery to load ratio, and non-availability of energy (Deshmukh and Deshmukh, 2008). In order to select an optimal combination of a HPWES to satisfy the load demand, evaluation may be carried on the basis of reliability and economy of power supply. The proposed methodology for evaluation of HPWES is described in the next section.

4.1. Reliability criteria based on DPSP technique

In this study, reliability of the system is expressed in terms of Deficiency of Power Supply Probability (DPSP) which is the probability that an insufficient power supply results when the hybrid system (PV array, wind power and energy storage) is unable to satisfy the load demand. The DPSP technique is considered to be the technical implemented criteria for sizing and evaluating a hybrid PV/wind system employing a battery bank. The technical model for hybrid system sizing is developed using the DPSP technique. The methodology used can be summarized in the following steps:

(a) If the power generated from the PV/wind system is greater than the load for a particular hour. In this case, the energy surplus is stored in the battery bank and the new state of charge is calculated using Eq. (19) until the full capacity is obtained; the remainder of the available energy is not used.
(b) When the energy demand of the load is greater than the available energy generated by the PV/wind system, the battery bank will be used to assure the load demand. In this case, the new state of charge at hour t is calculated using Eq. (20).

In case (a) when the state of charge of the battery bank reaches a maximum value, $SOC_{\max}$, the control system stops the charging process. The Excess Power Generated (EPG) is an important parameter, which gives the excess in power generated and unutilized by the system. This value can vary due to the variation of hourly average demand, insolation, wind velocity and state of charge of the battery bank. At hour t, the Excess Power Generated (EPG) can be expressed as follows:

$$EPG(t) = E_{Gen}(t) - [E_L(t)/\eta_{inv} + (SOC_{\max} - SOC(t-1))/\eta_B] \quad (22)$$

The Relative Excess Power Generated (REPG), expressed as the ratio of power excess to the sum of load demand during the considered period is calculated by the following equation:

$$\mathrm{REPG} = \sum_{t=1}^{T} \mathrm{EPG}(t) \Big/ \sum_{t=1}^{T} E_L(t) \tag{23}$$

In case (b), if the state of charge of the battery bank decreases to its minimum level, $SOC_{\min}$, the control system disconnects the load and that deficit called deficiency power supply (DPS) at hour t, can be expressed as:

$$\mathrm{DPS}(t) = E_L(t) - [E_{Gen}(t) + SOC(t-1) - SOC_{\min}]\eta_{inv} \tag{24}$$

The Deficiency of Power Supply Probability (DPSP), for a considered period T (1 year in this study), can be defined as the ratio of all the (DPS(t)) values for that period to the sum of the load demand. This can be defined as (Prasad and Natarajan, 2006):

$$\mathrm{DPSP} = \sum_{t=1}^{T} \mathrm{DPS}(t) \Big/ \sum_{t=1}^{T} E_L(t) \tag{25}$$

A DPSP of 1 means that the load will never be satisfied and the DPSP of 0 means that the load will be always satisfied. From the above-described situations, a program is developed in MATLAB to size the components for each configuration, for a particular DPSP specified by the user. The flow chart of HPWES model is illustrated in Fig. 3. In this program, $P_{PV,\min}$, $P_{PV,\max}$ and $P_{W,\min}$, $P_{W,\max}$ represent the lower and higher limits of the variation interval of the PV and wind generator rated power, respectively. ΔP_{pv} and ΔP_W represent the variation step of the PV and wind power, Δt the simulation step and ΔS_D is the step of storage days. In this study the maximum number of storage days, $NS_D = 3$.

The program input data set consists of hourly solar irradiation on a tilted plane, hourly mean values of ambient temperature and wind speed, desired DPSP, load power requirements during the year and specifications of the system devices. Using the developed program, a set of system configurations, which satisfy the system power reliability requirements, can be obtained. The optimal one is subsequently predicted on the basis of the minimum cost.

4.2. Cost analysis

It is judicious that economic analysis should be made while attempting to optimize the size of the proposed hybrid stand-alone system contributing to an acceptable unit price of power produced. The economic evaluation of the hybrid system has been made and the cost aspects have also been taken into account for optimization of the size of the system. Using the software developed, various costs namely, Total Net Present Cost (TNPC), Total Annualized Cost (TAC), and Break-Even Distance Analysis (BEDA; where the cost of the proposed hybrid stand-alone system breaks even with the cost of supplying the load with conventional grid power) are developed for system configurations considering the life period and replacement costs of the individual sub-systems.

4.2.1. Total Net Present Cost (TNPC)

The Total Net Present Cost (TNPC) analysis is an economic assessment of the cost for a number of alternatives considering all significant costs over the life period of each alternative, adding each option's costs for every year and discounting them back to a common base (present worth, PW). These costs can be categorized into two types: (a) recurring cost, e.g. maintenance cost for PV array and wind generator and (b) non-recurring cost, e.g. battery replacement cost. The conversion of recurring costs to present worth is as follows (Brown and Yanuck, 1985; Christopher et al., 2003):

$$\mathrm{PW}_{C_{rec}} = C_{rec} \frac{\left[\frac{1+e}{1+d}\right]\left\{\left[\frac{1+e}{1+d}\right]^{L_p} - 1\right\}}{\left[\frac{1+e}{1+d}\right] - 1} \tag{26}$$

where d and e are the interest and escalation rate, respectively. C_{rec} is the recurring cost and L_p is the system life period in years. The conversion of non-recurring cost to present worth is as follows:

$$\mathrm{PW}_{C_{non\text{-}rec}} = C_{non\text{-}rec} \frac{\left[\frac{1+e}{1+d_{adj}}\right]\left\{\left[\frac{1+e}{1+d_{adj}}\right]^{L_p} - 1\right\}}{\left[\frac{1+e}{1+d_{adj}}\right] - 1} \tag{27}$$

where d_{adj} is the adjusted interest rate given as follows, P is number of years between two successive payments for non-recurring costs and $C_{non\text{-}rec}$ is the non-recurring costs.

$$D_{adj} = \frac{(1+d)^P}{(1+e)^{P-1}} - 1 \tag{28}$$

The Total Net Present Cost (TNPC) may then be expressed as follows:

$$\mathrm{TNPC}(\$) = IC + \mathrm{PW}_{C_{rec}} + \mathrm{PW}_{C_{non-rec}} \tag{29}$$

where IC is the initial cost of the system components (including costs of civil work, installation and connections). All the parameters in the above equation are expressed in their present worth.

4.2.2. Total Annualized Cost (TAC)

The economical approach, according to the concept of the Total Annualized Cost (TAC), is developed to be one of the best indicators of economic profitability of system cost analysis in this study. According to the studied hybrid PV/wind system, the Total Annualized Cost of system (which is the sum of the annualized costs of each system component) is found by multiplying the Total Net Present

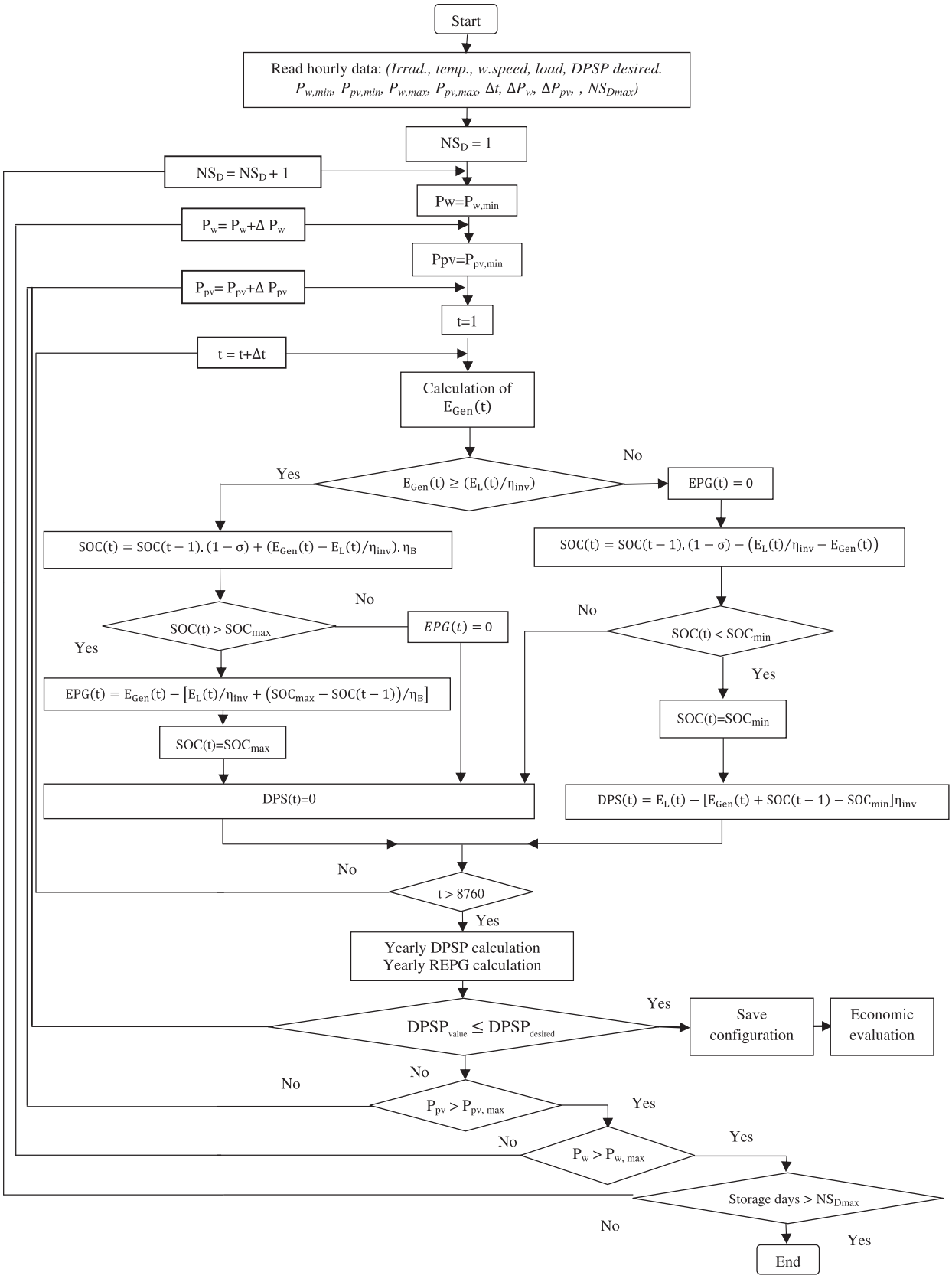

Fig. 3. Flow chart of the optimal sizing model.

Table 1
The costs and lifetime aspect for the system components.

Escalation rate e (%)	Interest rate d (%)	Lifetime (year)	Maintenance cost in the first year %	Unit Price (US$/W)	Component
4	8	25	1% of price	3.47	PV array[a]
		20	3% of price	3.000	Wind turbine[b]
		4	1% of price	0.210	Battery bank[a]
		10	0% of price	0.715	Inverter[a]

[a] http://www.solarbuzz.com.
[b] Mean value of the literature data.

Table 2
Specifications of the PV module.

P_{max} (W)	I_{max} (A)	V_{max} (V)	I_{sc} (A)	V_{oc} (V)	Type
55	3.16	17.4	3.40	21.7	Shell SM55

Table 3
Specifications of the wind turbine.

Tower high (m)	Cut-off speed V_F (m/s)	Rated speed V_R (m/s)	Cut-in speed V_C (m/s)	Rated power (W)	Type
10	25	12	3	400	AIR 403

Table 4
Specifications of the single battery.

DOD (%)	Charging efficiency	Voltage (V)	Nominal capacity (Ah)	Type
50	0.9	12	100	STECO 3000

Cost (TNPC) by the capital recovery factor (CRF). The TAC is defined as (Dalton et al., 2008).

$$\mathrm{TAC}(\$) = \mathrm{TNPC} \times \mathrm{CRF} \tag{30}$$

And the CRF (a ratio to calculate the present value of an annuity) is given by (Kaviani et al., 2009):

$$\mathrm{CRF}(d, L_p) = \frac{d(1+d)^{L_p}}{(1+d)^{L_p} - 1} \tag{31}$$

In which d is the interest rate and L_p is the system life period in years (25 years).

4.2.3. Break-Even Distance Analysis (BEDA)

As the economic viability of decentralized renewable energy systems is intimately tied to the distance of grid connection, a Break-Even Distance Analysis proves to be essential. This analysis determines how far the site of the stand-alone alternative energy system should be from the existing utility line so that the system is cost effective (breaks even) when compared to using conventional grid power. Thus, the optimum extended line distance is found by equating the Levelised Unit Electricity Cost (LUEC) for both hybrid system and grid power, the following equation is used (Nelson et al., 2006):

$$\mathrm{BEDA}\ (km) = \frac{\left[\mathrm{TAC} - \left(\mathrm{LUEC}_{grid} \times \sum_{t=1}^{8760} E_{Gen}(t)\right)\right]}{C_{ext} \times \mathrm{CRF}} \tag{32}$$

where BEDA is the Break Even Distance Analysis (km); LUEC_{grid} is the Levelised Unit Electricity Cost from the utility ($/kW h); C_{ext} is the cost of a line extension by the utility (an average cost of 50,000 $/km for Algiers utility is used in this study). (See Table 1)

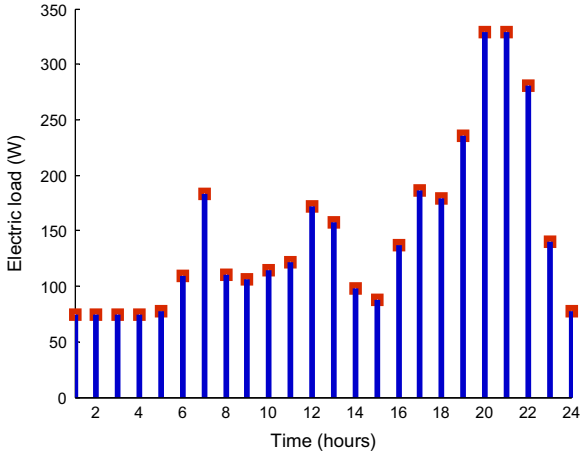

Fig. 4. Hourly load profile.

5. Results and discussion

5.1. Case study

The recommended methodology has been applied to analyze a stand-alone hybrid PV/wind energy system, which is designed to supply residential household located in the area of the Center for Renewable Energy Development (CDER) situated in Bouzaréah, Algeria (36°48′N, 3°1′E, 345 m). The technical characteristics of the PV module and wind turbine as well as the battery used in the studied project are listed in Tables 2–4. The load profile adopted in this research is that represented on Fig. 4. This hourly energy distribution is considered identical for every day of the year and corresponds to the load profile generally encountered in remote areas in Algeria.

Hourly data of solar irradiation on the horizontal plane, wind speed as well as ambient temperature, plotted in

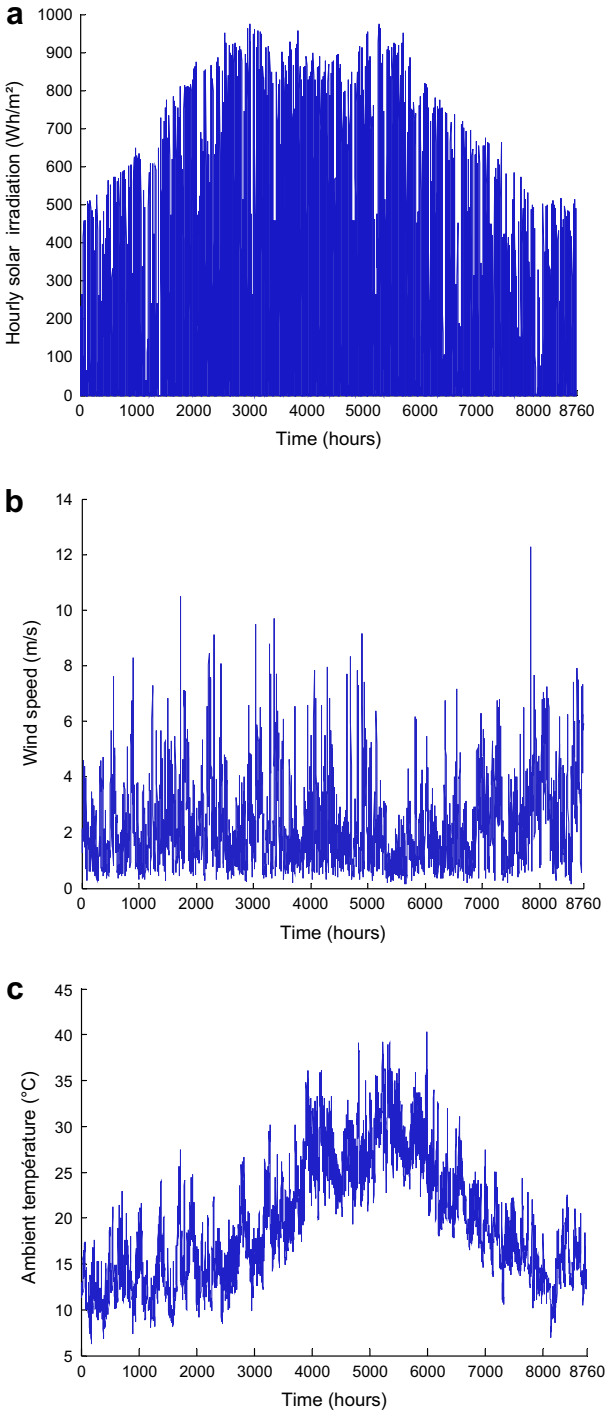

Fig. 5. Meteorological conditions for optimal design. (a) Solar irradiation on horizontal plane, (b) wind speed and (c) ambient temperature.

Fig. 5 during the year 2003, were recorded using a properly data-acquisition system installed at the CDER. The annual wind energy potential for Bouzaréah at 10 m height is 187 kW h/m^2 and the annual total solar radiation on the horizontal surface is 1626 kW h/m^2. On a comparative basis between the solar insolation and wind distribution of the site, there is a great scope for generating power from solar for longer periods in a year. Thus, the data recorded

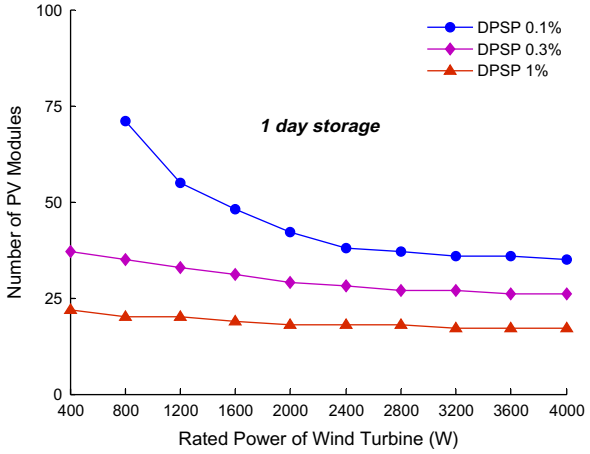

Fig. 6. System configurations for different DPSP for 1 day of autonomy of the battery bank.

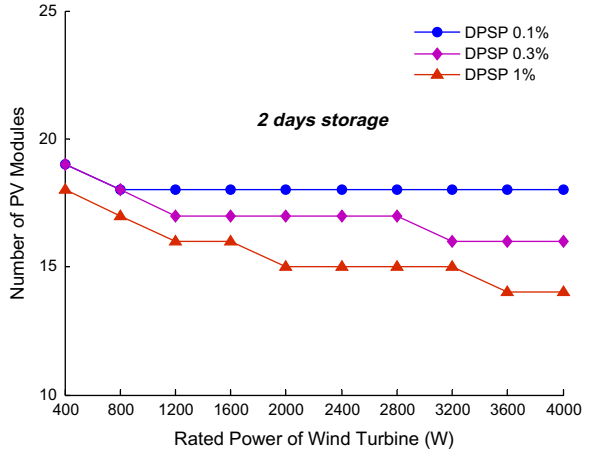

Fig. 7. System configurations for different DPSP for 2 days of autonomy of the battery bank.

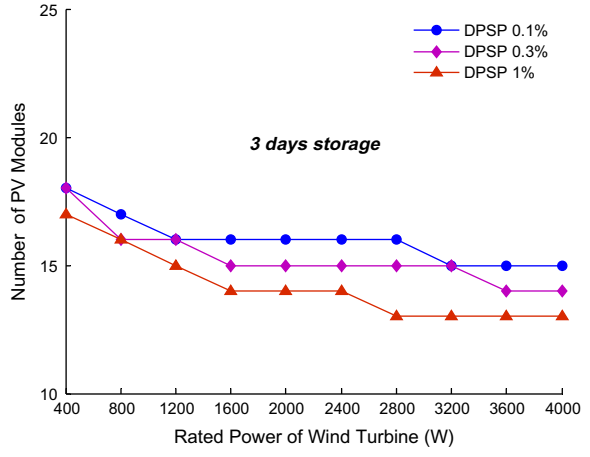

Fig. 8. System configurations for different DPSP for 3 days of autonomy of the battery bank.

are used in system unit sizing and the generation is assumed to keep constant in each hour interval.

5.2. Impact of power reliability on system configurations

The relationships between system reliabilities and system configurations are studied. Figs. 6–8 show the results of the relationship between system reliabilities or DPSP values and system configurations for different days of autonomy of the battery bank. Fig. 6 shows the relationships for a 1 day-storage battery bank. In this figure, the curves are hyperbolic nature. Each point of them represents a couple (Number of PV modules, wind turbine power) that guarantees the desired energy autonomy. In the case of a zero value of the DPSP, the corresponding curve is called curve of autonomy of the system: each point of this curve represents a combination which ensures the total autonomy of the system. The areas above the curves are also configurations that can ensure the required power reliability. It also shows that when the system reliability is higher; the system configuration (PV module and wind turbine power) is higher too for the same capacity of battery bank. A similar situation happens to the system for 2 and 3 days-storage battery bank (Figs. 7 and 8), but compared to the system with 1 day-storage battery bank, the PV module and wind turbine power are more moderate. It means the hybrid system with more batteries (3 days of storage capacity) can meet the load demand with less supply failure.

5.3. Impact of system configurations on the TNPC, TAC and BEDA

The configurations meeting different desired DPSP requirements under different battery capacities are obtained from the simulation results. After the technical criteria, the Total Net Present Cost (TNPC), Total Annualized Cost (TAC) and Break-Even Distance Analysis (BEDA) are utilized as the economic benchmarks. The simulation results are demonstrated and the relationships between TNPC, TAC, BEDA and power reliabilities as well as the system configurations are analyzed. In Figs. 9–14, the curves below in solid symbols show the results of the relationship between system reliabilities or DPSP values and system configurations for different days of autonomy of the battery bank (already presented in Figs. 6–8). Whereas, curves given by the hollow symbols in Figs. 9–14 represent the Total Net Present Cost (TNPC), Total Annualized Cost (TAC) and Break-Even Distance Analysis (BEDA) under different configurations. Obviously, one point with the minimum value of TNPC, TAC and BEDA occurs in each curve which means the best configuration for one certain DPSP value and one certain battery bank. This configuration is considered as the optimal one which meets the system reliability requirement with the lowest value of TNPC, TAC and BEDA. On the other hand, a meticulous examination into Figs. 9–14 shows that the lowest TNPC, TAC and BEDA are found when the capacity of wind turbine and the number of PV modules are both moderate. It is also shown that the TNPC, TAC and BEDA for 1 day battery storage are lower than 2 and 3 days for the desired DPSP of 0.3% and 1% for the studied case because batteries are much more expensive with a short lifespan.

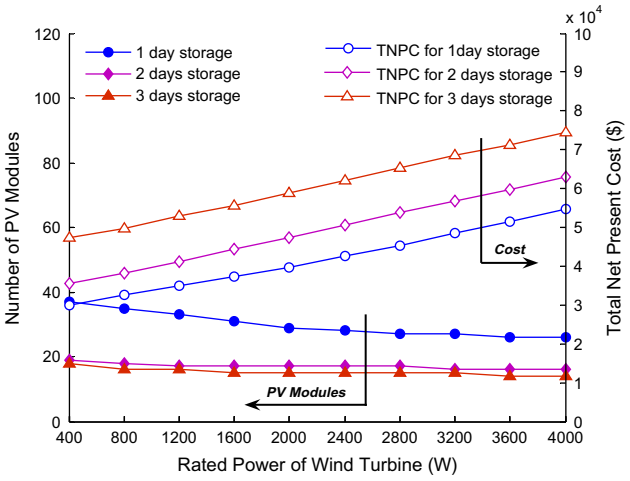

Fig. 9. System configurations and Total Net Present Cost for DPSP = 0.3%.

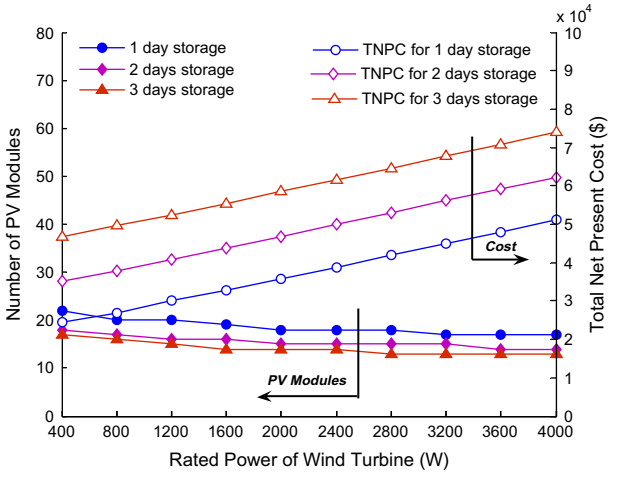

Fig. 10. System configurations and Total Net Present Cost for DPSP = 1%.

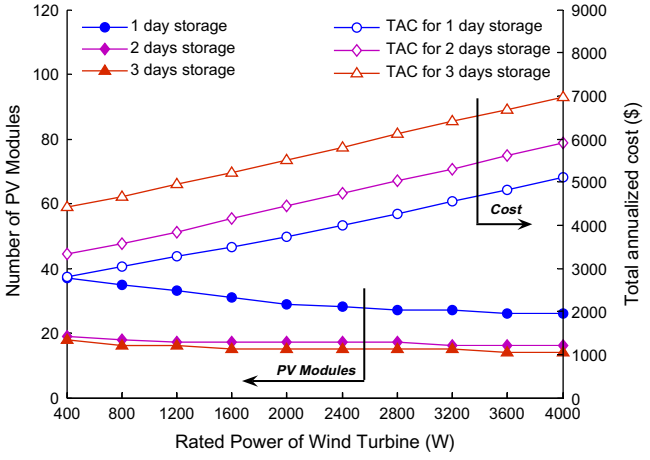

Fig. 11. System configurations and Total Annualized Cost for DPSP = 0.3%.

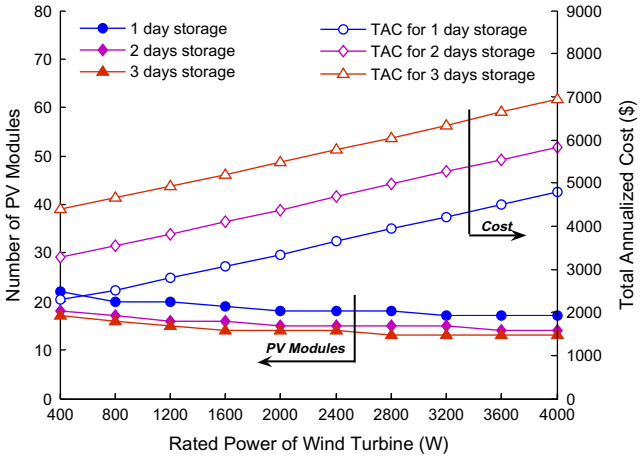

Fig. 12. System configurations and Total Annualized Cost for DPSP = 1%.

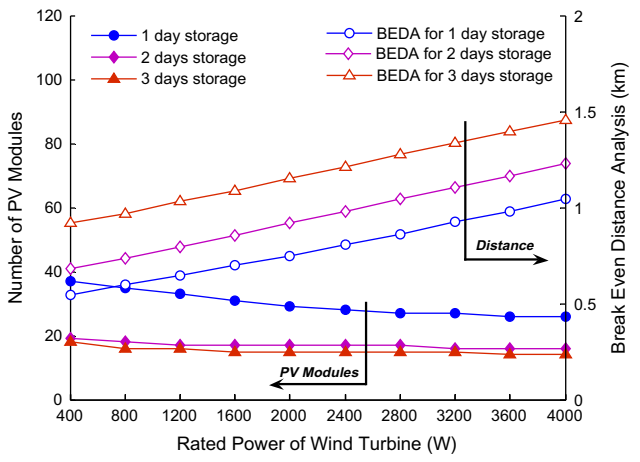

Fig. 13. System configurations and Break Even Distance Analysis for DPSP = 0.3%.

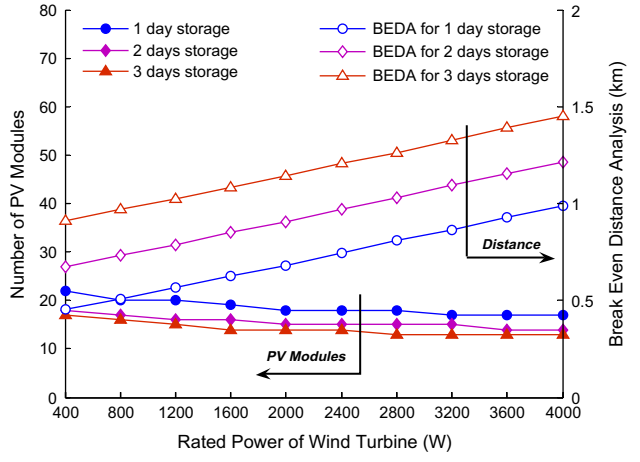

Fig. 14. System configurations and Break Even Distance Analysis for DPSP = 1%.

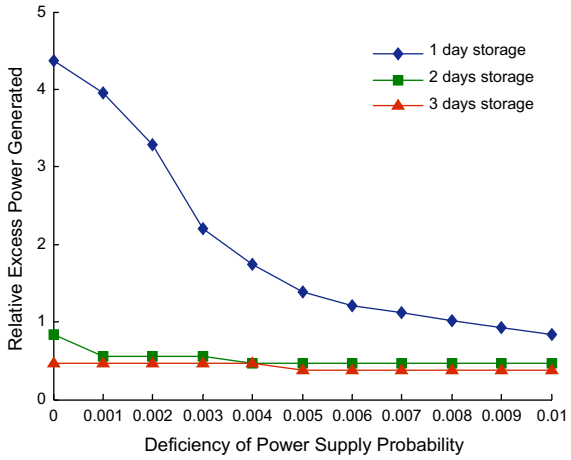

Fig. 15. REPG versus DPSP for different days of autonomy of the battery bank and for the optimum couples.

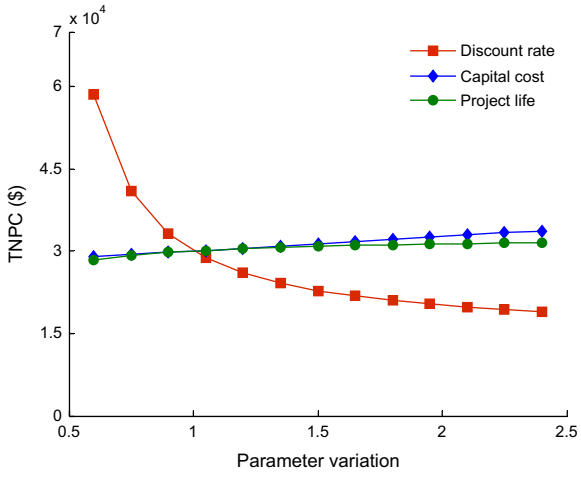

Fig. 16. Sensitivity of Total Net Present Cost for a hybrid PV/wind system.

5.4. Impact of power reliability and system configurations on the REPG

The variation of REPG with respect to DPSP for different days of autonomy of the battery bank is shown in Fig. 15. It is observed that REPG decreases with the increase in DPSP. It is estimated that for 1 day of autonomy of the battery bank, the REPG is around 437% for a DPSP of 0% (which corresponds to the total autonomy of the system) whereas it is 72% for a DPSP of 1%. imilarly for the case of 2 days of autonomy of the battery bank, the calculations show that the REPG is around 83% for a DPSP of 0% while it is 41% for a DPSP of 1%. A relative excess power of 43% is produced for a DPSP of 0% for 3 days of autonomy of the battery, while it is 29% for a DPSP of 1%. The high excess power produced, especially for 1 day of autonomy is due to the increasing of the number of PV panels and capacity of wind turbine (there is

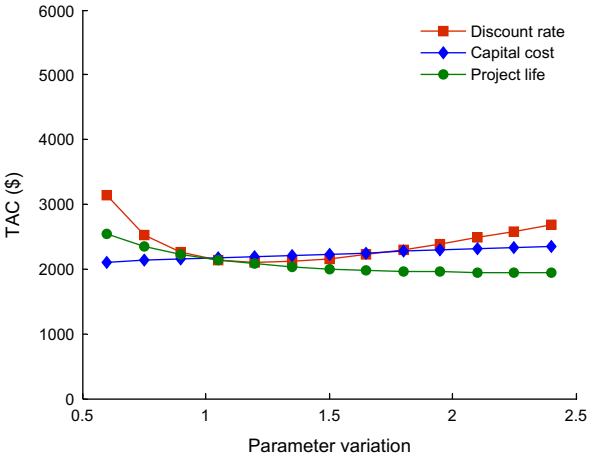

Fig. 17. Sensitivity of Total Annualized Cost for a hybrid PV/wind system.

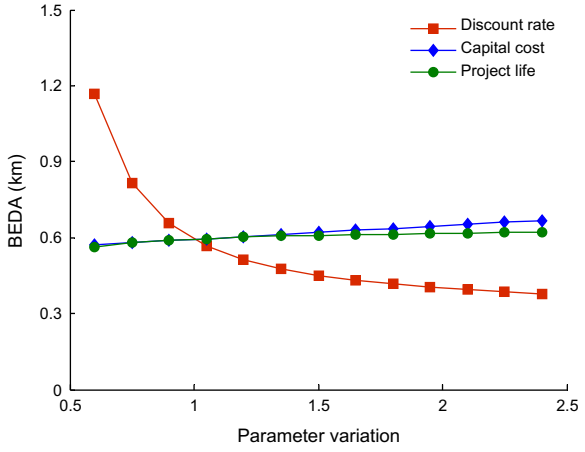

Fig. 18. Sensitivity of Break Even Distance Analysis for a hybrid PV/wind system.

a compromise between increasing the number of PV panels and capacity of wind turbine and increasing the number of batteries to meet the reliability requirements).

5.5. Sensitivity analysis

The effects on Total Net Present Cost (TNPC), Total Annualized Cost (TAC) and Break-Even Distance Analysis (BEDA) due to the changes in the discount rate, capital costs and project life has been studied for the hybrid system. The results of the sensitivity analysis are shown in Figs. 16–18. A discount rate of 8%, project life of 25 years and a direct capital cost of the hybrid PV/wind of $10,727 was considered as the central value. The parameter variation from 60% to 240% (0.6–2.4) was made for the sensitivity analysis. From Figs. 16 to 18, it can be seen that the TNPC, TAC and BEDA are sensitive to discount rates, direct capital costs and project life.

From Fig. 16, it can be seen that for a shorter discount rates, the TNPC values would be larger and are seen to be more sensitive. For longer discount rates, the TNPC is less sensitive. In the case of a shorter capital cost and project lifetime the TNPC is less sensitive and decrease slightly. For longer capital cost and project lifetime, the TNPC is less sensitive and increase faintly.

Fig. 17 shows the sensitivity of TAC to discount rates, capital cost as well as project lifetime. It can be seen that for a shorter and longer discount rates, the TAC values would be relatively larger and are seen to be more sensitive. In the case of a shorter project lifetime, the TAC values would be larger and are seen to be more sensitive. For a longer project lifetime, the TAC is less sensitive and depends on the major component replacements only. In addition there is a low sensitivity of TAC to capital cost for shorter and longer capital cost. Fig. 18 shows the sensitivity of BEDA to discount rates, capital cost as well as project lifetime. It can be seen that for a shorter discount rates, the BEDA values would be larger and are seen to be more sensitive. For longer discount rates, the BEDA is less sensitive. In the case of a shorter capital cost and project lifetime the BEDA is less sensitive and decrease lightly. For longer capital cost and project lifetime, the BEDA is less sensitive and increase faintly.

5.6. System optimal sizing result

The optimal sizing results for the DPSP of 0.3% and 1% (power reliability requirements) for different days of autonomy of the battery bank are shown in Table 5. For DPSP of 0.3%, TNPC is found to vary in the range of 30,040–47,232 $, TAC vary in the range of 2814.1–4424.6 $ and BEDA vary in the range 0.54–0.92 km depending on storage days. For DPSP of 1%, the range of TNPC is 24,405–46,856 $, the range of TAC is 2286.3–4389.4 $ and the range of BEDA is 0.45–0.91 km. It is clear from these results that the TNPC, TAC and BEDA for 1 day battery storage are lower than 2 and 3 days for the studied case

Table 5
Optimal sizing results for hybrid PV/wind system for DPSP = 0.3% and 1%.

DPSP = 1%			DPSP = 0.3%			Item
Three days storage	Two days storage	One day storage	Three days storage	Two days storage	One day storage	
17	18	22	18	19	37	N_{PV}
1	1	1	1	1	1	N_W
46,856	35,067	24,405	47,232	35,443	30,040	TNPC ($)
4389.4	3285.1	2286.3	4424.6	3320.2	2814.1	TAC ($)
0.91	0.67	0.45	0.92	0.68	0.54	BEDA (km)

because batteries are much more expensive with a short lifespan. Do not forget that these results may change for different types of PV modules, different wind turbines, different costs, and different types of batteries.

6. Conclusions

In this paper, an integrated photovoltaic/wind hybrid system optimization model, which utilizes the iterative optimization technique following the Deficiency of Power Supply Probability (DPSP), the Relative Excess Power Generated (REPG), the Total Net Present Cost (TNPC), the Total Annualized Cost (TAC) and Break-Even Distance Analysis (BEDA) for power reliability and system costs has been presented. The recommended model consists of six main parts: the submodel of the hybrid system, the technical submodel developed according to the Deficiency of Power Supply Probability (DPSP) technique for system reliability evaluation, the submodel witch permits the calculation of the Relative Excess Power Generated (REPG) and the economic submodels developed based on the concepts of Total Net Present Cost (TNPC), the Total Annualized Cost (TAC) and Break-Even Distance Analysis (BEDA) which are considered as a good indicators of economic profitability in the field of renewable energy. A set of configurations meeting the desired DPSP can be obtained by using the DPSP submodel. The configuration with the lowest TNPC, TAC and BEDA give the optimal one. Also, the developed model permits the calculation of the excess energy. So, the surplus energy produced could be used in the production of hydrogen from an electrolyzer for long-term energy storage, helping to improve the total efficiency of the hybrid system. Additionally, a sensitivity analysis was carried out in order to appreciate the most important parameters influencing the economic performances of the hybrid system.

A case study is conducted to analyze one hybrid project, which is designed to supply small residential household located in the area of the Center for Renewable Energy Development (CDER) situated in Bouzaréah, Algeria (36°48′N, 3°1′E, 345 m). The algorithm input data set consists of hourly solar irradiation on the horizontal plane, wind speed as well as ambient temperature recorded at Bouzaréah (Algeria) for the year 2003, the desired DPSP, load power requirements during the year and specifications of the system devices. The integrated PV/wind hybrid system is simulated by running the developed program and the relationships between system power reliability and system configurations on the one hand and system costs and system configurations on the other hand, have been studied. The optimal configurations of the hybrid system are determined in terms of different desired system reliability requirements (DPSP) and system costs. It is obvious from the obtained results that the TNPC, TAC and BEDA for 1 day battery storage are lower than 2 and 3 days for the studied case because batteries are much more expensive with a short lifespan.

References

Ai, B., Yang, H., Shen, H., Liao, X., 2003. Computer-aided design of PV/wind hybrid system. Renewable Energy 28, 1491–1512.

Belfkira, R., Zhang, L., Barakat, G., 2011. Optimal sizing study of hybrid wind/PV/diesel power generation unit. Solar Energy 85, 100–110.

Bernal-Agustín, J.L., Dufo-López, R., Rivas-Ascaso, D.M., 2006. Design of isolated hybrid systems minimizing costs and pollutant emissions. Renewable Energy 31, 2227–2244.

Borowy, B.S., Salameh, Z.M., 1996. Methodology for optimally sizing the combination of a battery bank and PV array in a wind/PV hybrid system. IEEE Transactions on Energy Conversion 11, 367–373.

Brown, J.R., Yanuck, R.R., 1985. Introduction to Life Cycle Costing. Fairmont Press, Englewood Cliffs, NJ.

Chedid, R., Rahman, S., 1997. Unit sizing and control of hybrid wind-solar power systems. IEEE Transactions on Energy Conversion 12, 79–85.

Chel, A., Tiwari, GN., 2010. Stand-alone photovoltaic (PV) integrated with earth to air heat exchanger (EAHE) for space heating/cooling of adobe house in New Delhi (India). Energy Conversion and Management 5, 1393–1409.

Chel, A., Tiwari, GN., 2011. A case study of a typical 232 kW_P stand-alone photovoltaic (SAPV) in composite climate of New Delhi (India). Applied Energy 88, 1415–1426.

Chel, A., Tiwari, GN., Chandra, A., 2009. Simplified method of sizing and life cycle cost assessment of building integrated photovoltaic system. Energy and Building 4, 11172–11180.

Chikh, M., Maafi, A., Malek, A., 2000. Etablissement d'un modèle Mathématique pour la fraction Diffuse de l'Irradiation Solaire en ALGERIE. Revue Energies Renouvelables. CHEMSS2000, 75–81.

Christopher et al., 2003. On the policy of photovoltaic and diesel generation mix for an off-grid site: East Malaysian perspectives. Solar Energy 74, 453–467.

Dalton, G.J., Lockington, D.A., Baldock, T.E., 2008. Feasibility analysis of stand-alone renewable energy supply options for a large hotel. Renewable Energy 33, 1475–1490.

Deshmukh, M.K., Deshmukh, S.S., 2008. Modeling of hybrid renewable energy systems. Renewable and Sustainable Energy Reviews 12, 235–249.

Diaf, S., Belhamelb, M., Haddadi, M., Louche, A., 2008a. Technical and economic assessment of hybrid photovoltaic/wind system with battery storage in Corsica Island. Energy Policy 36, 743–754.

Diaf, S., Notton, G., Belhamel, M., Haddadi, M., Louche, A., 2008b. Design and techno – economical optimization for hybrid PV/wind system under various meteorological conditions. Applied Energy 85, 968–987.

Dufo-López, R., Bernal-Agustín, J.L., 2008. Multi-objective design of PV–wind–diesel– hydrogen–battery systems. Renewable Energy 33, 2559–2572.

Ekren, O., Ekren, B.Y., 2010. Size optimization of a PV/wind hybrid energy conversion system with battery storage using simulated annealing. Applied Energy 87, 592–598.

Esen, H., Inalli, M., Esen, M., 2006. Technoeconomic appraisal of a ground source heat pump system for a heating season in eastern Turkey. Energy Conversion and Management 47, 1281–1297.

Esen, H., Inalli, M., Esen, M., 2007. A techno-economic comparison of ground-coupled and air-coupled heat Pump system for space cooling. Building and Environment 42, 1955–1965.

Habib, M.A., Said, S., El-Hadidy, M.A., Al-Zaharna, I., 1999. Optimization procedure of a hybrid photovoltaic wind energy system. Energy 24, 919–929.

Iqbal, M., 1983. An introduction to solar radiation. Academic Press, Canada, ISBN 0-12-373752–4.

Kaabeche, A., Belhamel, M., Ibtiouen, R., Moussa, S., Benhadadi, M.R., 2006. Optimisation d'un système hybride (Eolien–Photovoltaïque) totalement autonome. Revue des Energies Renouvelables 9, 199–209.

Kaabeche, A., Belhamel, M., Ibtiouen, R., 2010. Sizing optimization of grid-independent hybrid photovoltaic/wind power generation system. Energy 36, 1214–1222.

Karaki, SH., Chedid, R.B., Ramadan, R., 1999. Probabilistic performance assessment of autonomous solar-wind energy conversion systems. IEEE Transactions on Energy Conversion 14, 766–772.

Kaviani, A.K., Riahy, G.H., Kouhsari, S.H.M., 2009. Optimal design of a reliable hydrogen-based stand-alone wind/PV generating system, considering component outages. Renewable Energy 34, 2380–2390.

Klucher, T.M., 1979. Evaluation of models to predict insolation on tilted surfaces. Solar Energy 23, 111–114.

Kolhe, M., Agbossou, K., Hamelin, J., Bose, T.K., 2003. Analytical model for predicting the performance of photovoltaic array coupled with a wind turbine in a stand-alone renewable energy system based on hydrogen. Renewable Energy 28, 727–742.

Markvar, T., 2000. Solar Electricity, second ed. J. Wiley & Sons.

Markvart, T., 1996. Sizing of hybrid PV-wind energy systems. Solar Energy 59, 277–281.

Mehleri, E.D., Zervas, P.L., Sarimveis, H., Palyvos, J.A., Markatos, N.C., 2010. Determination of the optimal tilt angle and orientation for solar photovoltaic arrays. Renewable Energy 35, 2468–2475.

Nelson, D.B., Nehrir, M.H., Wang, C., 2006. Unit sizing and cost analysis of stand-alone hybrid wind/PV/fuel cell power generation system. Renewable Energy 31, 1641–1656.

Notton, G., Lazarov, V., Stoyanov, L., 2010. Optimal sizing of a grid-connected PV system for various PV module technologies. Renewable Energy 35, 541–554.

Posadillo, R., López Luque, R., 2009. Evaluation of the performance of three diffuse hourly irradiation models on tilted surfaces according to the utilizability concept. Energy Conversion and Management 50, 2324–2330.

Prasad, A.R., Natarajan, E., 2006. Optimization of integrated photovoltaic–wind power generation systems with battery storage. Energy 31, 1943–1954.

Tina, G., Gagliano, S., Raiti, S., 2006. Hybrid solar/wind power system probabilistic modeling for long-term performance assessment. Solar Energy 80, 578–588.

Wen, J., Zheng, Y., Donghan, F., 2009. A review on reliability assessment for wind power. Renewable and Sustainable Energy Reviews 13, 2485–2494.

Yang, H.X., Burnett, L., Lu, J., 2003. Weather data and probability analysis of hybrid photovoltaic–wind power generation systems in Hong Kong. Renewable Energy 28, 1813–1824.

Yang, H., Lu, L., Zhou, W., 2007. A novel optimization sizing model for hybrid solar-wind power generation system. Solar Energy 81, 76–84.

Yang, H.X., Zhou, W., Lu, L., Fang, Z.H., 2008. Optimal sizing method for stand-alone hybrid solar–wind system with LPSP technology by using genetic algorithm. Solar Energy 82, 354–367.

Yokoyama, R., Ito, K., Yuasa, Y., 1994. Multi-objective optimal unit sizing of hybrid power generation systems utilizing PV and wind energy. Journal of Solar Energy Engineering 116, 167–173.